

Evidence for a Multivalent Interaction of Symmetrical, N-Linked, Lidocaine Dimers with
Voltage-Gated Na⁺ Channels.

J. A. M. Smith, S. M. Amagasu, J. Hembrador, S. Axt, R. Chang, T. Church, C. Gee, J. R.
Jacobsen, ¹T. Jenkins, E. Kaufman, N. Mai, R.G. Vickery.

Theravance Inc., 901 Gateway Blvd., South San Francisco CA 94080, USA

Running Title: Interaction of lidocaine dimers with VGSCs

Author for correspondence:

Jacqueline Smith

Theravance Inc.,

901 Gateway Blvd.,

South San Francisco CA 94080

Tel: 650-808-6415

Fax: 650-808-6886

E-mail: jsmith@theravance.com

Number of text pages: 26

Number of tables: 4

Number of figures: 8

Number of references: 40

Number of words:

Abstract – 250

Introduction – 706

Discussion – 1500

Abbreviations: C₂, *n*-ethylene; C₃, *n*-propylene; C₄, *n*-butylene; C₅, *n*-pentylene; C₆, *n*-hexylene; DMEM, Dulbecco's Modified Eagle's Medium; MEM, minimum essential medium; FIU, fluorescence intensity units; FLIPR^R, fluorimetric imaging plate reader; FMP, FLIPR^R membrane potential assay kit; HBSS, Hank's balanced salt solution; VGSC, voltage-gated Na⁺ channel

Abstract

The interaction of symmetrical lidocaine dimers with voltage-gated Na⁺ channels (VGSCs) was examined using a FLIPR[®] membrane potential assay and voltage-clamp. The dimers, in which the tertiary amines of the lidocaine moieties are linked by an alkylene chain (2 to 6 methylene units), inhibited VGSC activator-evoked depolarization of cells heterologously-expressing rNa_v1.2a, hNa_v1.5 and rNa_v1.8, with potencies 10- to 100-fold higher than lidocaine (compound **1**). The rank order of potency (C₄ (compound **4**) > C₃ (compound **3**) ≥ C₂ (compound **2**) = C₅ (compound **5**) = C₆ (compound **6**) >> compound **1**) was similar at each VGSC. Compound **4** exhibited strong use-dependent inhibition of hNa_v1.5 with pIC₅₀ values < 4.5 and 6.0 for tonic and phasic block, respectively. Coincubation with local anesthetics but not tetrodotoxin attenuated compound **4**-mediated inhibition of hNa_v1.5. These data suggest that the compound **4** binding-site(s) is identical, or allosterically-coupled, to the local anesthetic receptor. The dissociation rate of the dimers from hNa_v1.5 was dependent upon the linker length, with a rank order; compound **1**>compound **5**=compound **6**>compound **2**>>compound **3**. The observation that both the potency and dissociation rate of the dimers was dependent upon linker length is consistent with a multivalent interaction at VGSCs. hNa_v1.5 VGSCs did not recover from inhibition by compound **4**. However, 'chase' with free local anesthetic site inhibitors increased the rate of dissociation of compound **4**. Collectively these data support the hypothesis that compound **4** simultaneously occupies two binding sites on VGSCs, both of which can be bound by known local anesthetic site inhibitors.

Introduction

VGSCs are transmembrane protein complexes that increase Na^+ permeability in response to membrane depolarization. Mammalian VGSCs consist of a pore-forming or α subunit, which is sufficient for functional channel expression, associated with one or more auxiliary β subunits. The α subunit consists of four homologous domains (D1-D4) each of which has six transmembrane alpha helices (S1-S6) (Catterall, 2000). The VGSC is thought to be organized as a pseudotetramer with the S6 segments lining the inner surface of the channel pore (Sato et al., 2001). At least nine genes encoding VGSC α subunits have been identified ($\text{Na}_v1.1$ - $\text{Na}_v1.9$), which can be differentiated on the basis of their tissue distribution profiles, biophysical and/or pharmacological properties (Goldin et al., 2000).

In the plasma membrane, VGSC's interconvert between multiple conformational states (e.g. closed/resting, open, inactivated) in response to changes in membrane potential (Hille, 2001). The affinity of local anesthetics, which confer their activity by inhibiting the conduction of Na^+ ions through VGSCs and, thereby, action potential initiation/propagation in excitable tissues, depends upon the conformational state of the channel (Ragsdale et al., 1991). Local anesthetics bind to non-resting i.e. open/inactivated states with higher affinity than to resting states (Hondeghe and Katzung, 1977; Bean et al., 1983). The higher affinity of local anesthetics for the non-resting states is manifest as use-dependence.

Receptors, ion channels and enzymes which possess multiple binding sites, due to symmetry, pseudosymmetry, or the presence of unrelated auxiliary sites, may be targeted pharmacologically with dimeric ligands. Such an approach seeks to tether two ligands with a linker that can orient the ligands to bind the target simultaneously (Kiessling et al., 2000; Wright and Usher, 2001). The simultaneous occupation of two distinct concavities on a protein by such a bivalent ligand can confer upon it enhanced affinity, duration of action and/or subtype selectivity, relative to its component monomeric ligand(s) (Mammen et al.,

1998). The critical parameters that control these properties are linker length, linker geometry and/or composition, ligand identity and ligand attachment points.

Bivalent ligand design has been used successfully for G-protein-coupled receptors such as β -adrenergic (Kizuka and Hanson, 1987), kappa opioid (Portoghese et al., 1988), muscarinic acetylcholine (Christopoulos et al., 2001), 5-HT_{1A/D} (LeBoulluec et al., 1995) and 5-HT_{1B/1D} (Halazy et al., 1996) receptors. Similar studies also have been undertaken for voltage-gated calcium channels (Joslyn et al., 1988); SK_{Ca} (Galanakis et al., 1996), nicotinic (Rosini et al., 1999), and cyclic nucleotide-gated (Kramer and Karpen, 1998) ion channels.

To the best of our knowledge, this approach has not been applied previously to VGSCs although a number of structural features of VGSCs are consistent with the application of multivalent ligand design. In addition to the putative tetrameric organization of their four homologous domains, VGSCs also have six distinct binding sites for small molecules and peptide toxins (Cestele and Catterall, 2000). Based on the results of site-directed mutagenesis studies it has been proposed that the S6 segments contribute to a domain-interface binding site for local anesthetics, analogous to that for antagonist binding in L-type Ca²⁺ channels (Hockerman et al., 1997). Thus, amino acid residues in D1-S6 (Nau et al., 1999; Yarov-Yarovoy et al., 2002); D3-S6 (Wang et al., 2000 ; Yarov-Yarovoy et al., 2001) and D4-S6 (Ragsdale et al., 1996) have been proposed to participate in local anesthetic binding. However, other groups (Bennett et al., 1995; Kuroda et al., 1996, 2000) have proposed that, in addition to the D4-S6 conserved local anesthetic receptor, lidocaine also interacts with the D3-D4 cytoplasmic linker, which forms part of the inactivation domain. Further, the existence of two independent binding sites for local anesthetics or small molecule VGSC inhibitors has been postulated (Lee-Son et al., 1992; Mujtaba et al., 2001, 2002; Leuwer et al., 2004).

In the present study, the interaction of a series of symmetrical, *N*-linked lidocaine dimers, in which the nitrogens of each lidocaine moiety are tethered by an unsubstituted alkylene chain

(2 to 6 methylene units) (Figure 1), with tetrodotoxin-sensitive ($\text{Na}_v1.2a$), tetrodotoxin-resistant ($\text{Na}_v1.8$) and cardiac ($\text{Na}_v1.5$) VGSC subtypes was examined. CHO-K1, 293-EBNA and F-11 cells stably-transfected with r $\text{Na}_v1.2a$ (r $\text{Na}_v1.2a$ -CHO), h $\text{Na}_v1.5$ (h $\text{Na}_v1.5$ -293-EBNA) and r $\text{Na}_v1.8$ (r $\text{Na}_v1.8$ -F-11), respectively, were used for FLIPR[®]-based assays of membrane potential and whole cell voltage-clamp recordings. To characterize the interaction of dimers with native tetrodotoxin-resistant VGSCs, primary cultures of rat dorsal root ganglia neurons were used.

Materials and Methods

Cell Culture of rNa_v1.2a-CHO, hNa_v1.5-293-EBNA and rNa_v1.8-F-11 cells

rNa_v1.2a-CHO cells were obtained under license from Dr. W. Catterall (University of Washington, Seattle, WA) and grown in RPMI Medium 1640 containing 1 mM L-glutamine, supplemented with 5 % heat inactivated fetal bovine serum, 200 µg/ml geneticin and 50 units/ml penicillin-50 µg/ml streptomycin. hNa_v1.5-293-EBNA cells were obtained under license from Dr. A. O. Grant (Duke University, Chapel Hill, NC) and grown in DMEM containing L-glutamine, supplemented with 5 % heat inactivated fetal bovine serum, 50 µg/ml hygromycin, additional 1mM L-glutamine, and 50 units/ml penicillin-50 µg/ml streptomycin.

F-11 cells were obtained under license from Dr. M. Fishman (Harvard Medical School, Cambridge, MA). Untransfected F-11 and rNa_v1.8-F-11 cells were grown in Ham's F12 Medium containing L-glutamine supplemented with 20 % heat inactivated fetal bovine serum, 1 % HAT (100 µM hypoxanthine, 0.4 µM aminopterin and 16 µM thymidine), additional 1 mM L-glutamine and 50 units/ml penicillin-50 µg/ml streptomycin, in the absence and presence of 200 µg/ml geneticin, respectively. All cell lines were grown routinely as monolayers in an atmosphere of 95% O₂/5% CO₂ at 37°C.

For FLIPR^R studies, cells were seeded into black-walled, clear-bottom 96-well microtiter plates coated with poly-D-lysine (Becton-Dickinson, Franklin Lakes, NJ). rNa_v1.2a-CHO and hNa_v1.5-293-EBNA cells were seeded at optimized concentrations of 50 x 10³ cells/well and 20 x 10³ cells/well, respectively and used for assay approximately 3 hours later. rNa_v1.8-F-11 cells were plated at an optimized concentration of 22 x 10³ cells/well and incubated overnight prior to assay. For electrophysiological studies cells were plated onto poly-D-lysine-coated (100 µg/ml) coated glass coverslips at a density that enabled isolated cells to

be selected for voltage-clamp recordings and maintained under 95%/5% O₂/CO₂ at 37°C for 12-48 h prior to recording.

Measurement of Membrane Potential using the FLIPR[®]

Membrane potential in rNa_v1.2a-CHO, hNa_v1.5-293-EBNA and rNa_v1.8-F-11 cell lines was monitored using a fluorescent membrane potential sensitive (FMP) dye (Molecular Devices Corporation, Sunnyvale, CA) and FLIPR[®] as described previously by Vickery et al., 2004. Membrane depolarization, or hyperpolarization, of FMP dye-loaded cells produces an increase, or decrease, respectively, in fluorescence emission.

Briefly, cells were incubated with FMP dye under the conditions indicated in parentheses: rNa_v1.2a-CHO (50 min, 22°C), hNa_v1.5-293-EBNA (35 min, 22°C), rNa_v1.8-F-11 (45 min, 37°C). For the final 30 min of the dye loading period, cells were incubated in the absence (i.e. control), or presence, of increasing concentrations of antagonists. The plates then were placed on the FLIPR[®] and cell fluorescence monitored (λ_{ex} = 488 nm, λ_{em} : relevant emission filter provided by Molecular Devices) before, and after, the addition of HBSS-HEPES buffer containing the appropriate concentrations of VGSC activators. Activation of Na⁺ channels in rNa_v1.2a-CHO, hNa_v1.5-293-EBNA and rNa_v1.8-F-11 cells was achieved using veratridine (20 μ M) alone; veratridine (20 μ M) plus deltamethrin (3 μ M); and veratridine (20 μ M) plus deltamethrin (20 μ M), respectively. Fluorescence emission was monitored for 15 s prior to the addition of stimulus buffer, to establish a baseline, and then for 4 min following the addition. For rNa_v1.8-F-11 all additions of Na⁺ channel activators were made at 37°C on the FLIPR[®]. To ensure that the temperature was stable during the recording period, rNa_v1.8-F-11 cells were pre-equilibrated for 15 min in the FLIPR[®] prior to activator addition. F-11 cells express an endogenous tetrodotoxin-sensitive VGSC therefore, recombinant rNa_v1.8-F-11 cells were co-incubated with 300 nM tetrodotoxin (final assay concentration following

activator addition) to isolate $rNa_v1.8$ -mediated depolarizations. A panel of control compounds, including tetrodotoxin, lidocaine, bupivacaine and mexiletine was included in all experiments to confirm the stability of VGSC expression in the respective cell lines.

10 mM stock solutions of all compounds were prepared in 100% DMSO, with the exception of veratridine and deltamethrin, for which a 40 μ M veratridine stock solution in 100% EtOH and 80 μ M deltamethrin stock solution in 100% DMSO were prepared.

FLIPR[®] FMP Assay Data Analysis

FLIPR[®] data points were taken every 2 s. For data analysis, peak fluorescence (fluorescence intensity units) was measured using the FLIPR[®] software. Peak values were exported into EXCEL and then into GraphPad Prism 3.0 (San Diego, CA). Concentration-response curves were fitted to a four parameter sigmoidal function, with a variable slope, using GraphPad Prism (GraphPad Prism Software Inc., CA). Data were analysed with the assumption that a single dimer molecule bound to, and blocked, one VGSC. One-way ANOVA and post-hoc Tukey's multiple comparison tests, were conducted using GraphPad/Prism. Data represent mean \pm s.d., of at least 3 independent experiments. All experiments were conducted at least in duplicate.

Preparation of Neonatal Rat Dorsal Root Ganglia Primary Cultures.

Post-natal day 1-2 Sprague Dawley rats were sacrificed by CO₂ inhalation, in accordance with the IACUC regulations, and dorsal root ganglia from all spinal levels were dissected. Primary cultures of neonatal rat dorsal root ganglia cells were prepared according to a modification of the procedure described previously (Vickery *et al.*, 1998). Briefly, dorsal root ganglia were dispersed using a combination of enzymatic treatments and mechanical trituration. Dorsal root ganglia were incubated with collagenase (0.06%, 25 min at 37°C) and

then trypsin (0.125%, 15 min at 37°C) prior to trituration with fire-polished glass pasteur pipettes in the presence of 0.01% DNase. The final cell suspension was resuspended in Dulbecco's Modified Eagles Medium (DMEM)/F12 containing 10% fetal bovine serum, 100 ng/ml NGF and 10 μ M arabinoside C (to suppress the growth of non-neuronal cells) and plated onto poly-D-lysine (10 μ g/ml) and laminin (5 μ g/ml) coated 13 mm glass coverslips at a density which enabled isolated cells to be selected for voltage-clamp recordings. Cells were maintained at 37°C in an atmosphere of 95%/5% O₂/CO₂ for 1-2 days.

Whole Cell Voltage-Clamp

Patch pipettes were manufactured from glass capillary tubing (borosilicate-thin wall, OD 1.5 mm, ID 1.17 mm) (Warner Instruments Corporation, Hamden, CT) using a P-97 Flaming-Brown pipette puller (Sutter Instrument Co., Novato, CA) and polished with a microforge (Narishige, East Meadow, NY). The measured pipette resistance was between 1 and 3 M Ω , when placed in the bath. The reference electrode consisted of a Ag/AgCl pellet placed in the external solution. The potential between the two electrodes was adjusted for zero current flow, prior to the establishment of a seal. rNa_v1.2a-CHO and hNa_v1.5-293-EBNA cells were superfused with an extracellular solution containing (mM): NaCl 140, KCl 4.7, MgCl₂ 2.6, glucose 11 and HEPES 5, pH 7.4 at room temperature. For recording rat dorsal root ganglia tetrodotoxin-resistant currents, the extracellular solution contained (mM): choline 60, NaCl 65, MgCl₂ 5, CaCl₂ 1, KCl 5, Glucose 10, HEPES 10, (pH adjusted to 7.4 with NaOH) and tetrodotoxin (300 nM). For all cell types, recording pipettes were filled with an internal solution containing (mM): CsF 120, Cs-EGTA 20, CaCl₂ 1, MgCl₂ 1, NaCl 15, and HEPES 10, pH 7.2. Cells were voltage-clamped, in the whole cell configuration, using an Axopatch 200B amplifier (Axon Instruments, Inc., Union City, CA). Series resistance and cell capacitance were balanced using the amplifier's internal circuitry. Access resistances were not recorded

routinely. However, precautions were undertaken in order to minimize command voltage errors. Only cells with peak currents less than 5 nA were used. Further, the amplifier's series resistance compensation circuitry was routinely adjusted to 60-80% to further ensure proper voltage control. Both current and voltage waveforms were filtered at 5 kHz, digitized at 20 kHz and stored for offline analysis. Voltage command protocols were generated by pClamp 8.0 (Axon Instruments) software driving either an Axon Digidata 1200 or 1320 digitizer.

Na⁺ currents were elicited by depolarizing the membrane potential to either -20 or 0 mV for 10 ms, from an appropriate holding potential. Data were stored in an Axon Binary File format. The standard holding and test potentials for the different channels are indicated in parentheses: rNa_v1.2a (-100mV, 0 mV); hNa_v1.5 (-120 mV, -20 mV) and rat dorsal root ganglia tetrodotoxin-resistant (-90 mV, 0 mV). Briefly, after stabilization of the voltage-clamp, Na⁺ current magnitude was monitored, at a frequency of 0.2 Hz, for a period of one minute. The compound was applied in the absence of any depolarizations for 3 min duration. Then, in the continuous presence of compound, a 5 Hz train of 200 pulses (10 ms duration) to the appropriate test potential, was applied. Peak current amplitudes for the first and 200th depolarizations were determined using pCLAMP and then normalized to the initial current in the absence of compound. The degree of inhibition of the first and last depolarizations represents the degree of tonic and phasic block, respectively (Weiser et al., 1999).

For rat dorsal root ganglia tetrodotoxin-resistant Na⁺ currents, in the absence of compound, there was a 23 ± 2 % (mean \pm sem, n = 6 cells) reduction in the magnitude of the final pulse in the 5 Hz train at the high stimulus frequency. To correct for this decrement in current amplitude, which occurs in the absence of drug, each normalized data point, in the presence of drug, was divided by that in the absence.

Concentration-response curves of normalized current amplitude against compound concentrations were constructed (n = 3 or more cells for each point) and the data fitted to a

four parameter sigmoidal function using Origin^R (OriginLab Corp., Northampton, MA). The upper and lower asymptotes were constrained to 1 and 0, respectively.

Compound dissociation rates from hNa_v1.5 and rNa_v1.2a VGSCs were determined. After stabilization of the voltage-clamp, Na⁺ current magnitude was monitored, at a frequency of 0.2 Hz, for a period of one min. hNa_v1.5-293-EBNA or rNa_v1.2a-CHO cells then were exposed to the specified concentration of lidocaine or dimer according to the protocols described above. At the end of the 5 Hz stimulus train the compound was washed out by continuous perfusion with extracellular buffer and current magnitude monitored at a frequency of 0.2 Hz for an additional 10 min. Current amplitudes were normalized to the initial current in the absence of compound and plots of normalized current amplitude against time constructed (n = 3 or more cells for each point). Data (from time of compound washout) were fitted to a single exponential decay function using Origin^R (OriginLab Corp., Northampton, MA).

Unpaired t-test or one-way ANOVA and post-hoc Dunnett's test were conducted using GraphPad/Prism. Data represent mean \pm s.d., for at least 3 cells.

Materials

Cell culture media and supplements were obtained from Gibco Invitrogen (Invitrogen, Carlsbad, CA). The following materials were obtained from the sources indicated in parentheses: Pfx8 (Promega, Madison, WI), TRIZOL reagent (Invitrogen, Carlsbad, CA); fetal bovine serum (Hyclone, Logan, UT); FMP (Molecular Devices, Sunnyvale, CA). All other reagents were obtained from Sigma-Aldrich (Sigma-Aldrich Corp., St. Louis, MO).

The following drugs were obtained from the commercial sources indicated in parentheses: deltamethrin (RU29974) (Dr. Ehrenstorfer GmbH, Augsburg, GDR); veratridine, tetrodotoxin (Sigma-Aldrich Corp., St. Louis, MO). Mexiletine, pimozide, bupivacaine, 4030W92, lamotrigine, compound **1** (lidocaine, 2-Diethylamino-N-(2,6-dimethyl-phenyl)-acetamide),

compound **2** (*N*-(2,6-Dimethyl-phenyl)-2-[(2-[(2,6-dimethyl-phenylcarbamoyl)-methyl]-methyl-amino)-ethyl]-methyl-amino]-acetamide), compound **3** (*N*-(2,6-Dimethyl-phenyl)-2-[(3-[(2,6-dimethyl-phenylcarbamoyl)-methyl]-methyl-amino)-propyl]-methyl-amino]-acetamide), compound **4** (*N*-(2,6-Dimethyl-phenyl)-2-[(4-[(2,6-dimethyl-phenylcarbamoyl)-methyl]-methyl-amino)-butyl]-methyl-amino]-acetamide, THR-170148), compound **5** (*N*-(2,6-Dimethyl-phenyl)-2-[(5-[(2,6-dimethyl-phenylcarbamoyl)-methyl]-methyl-amino)-pentyl]-methyl-amino]-acetamide), compound **6** (*N*-(2,6-Dimethyl-phenyl)-2-[(6-[(2,6-dimethyl-phenylcarbamoyl)-methyl]-methyl-amino)-hexyl]-methyl-amino]-acetamide), compound **7** (*N*-(2,6-Dimethyl-phenyl)-2-[methyl-(4-methylamino-butyl)-amino]-acetamide), compound **8** (*N*-(2,6-Dimethyl-phenyl)-2-[methyl-(4-(methyl-methylcarbamoylmethyl-amino)-butyl)-amino]-acetamide) and compound **9** (*N*-(4-[(2,6-Dimethyl-phenylcarbamoyl)-methyl]-methyl-amino)-butyl)-*N*-methyl-3-phenyl-propionamide) were prepared by the Theravance Inc. Medicinal Chemistry Department for Theravance Inc. research purposes only.

Results

Inhibition of Na⁺ channel activator-evoked depolarization of rNa_v1.2a-CHO, hNa_v1.5-293-EBNA and rNa_v1.8-F11 cells by lidocaine dimers is dependent upon the length of the tether.

The interaction of the dimers with specific VGSC subtypes initially was examined using rNa_v1.2a-CHO, hNa_v1.5-293-EBNA and rNa_v1.8-F-11 recombinant cell lines and a novel FLIPR[®] membrane potential sensitive dye assay (Vickery et al., 2004). tetrodotoxin produced a concentration-dependent inhibition of Na⁺ channel activator-evoked depolarization of rNa_v1.2a-CHO, hNa_v1.5-293-EBNA and rNa_v1.8-F-11 cells with pIC₅₀ values as expected for inhibition of Na_v1.2a, Na_v1.5 and Na_v1.8 Na⁺ channels, respectively (see Table 1). Lidocaine, and the dimers, also produced a concentration-dependent inhibition of activator-evoked depolarization in each cell type (Table 1). The potencies of the dimers were dependent upon the length of the linker and ranged from 10 to ≥ 100-fold higher than that of lidocaine (p < 0.001, Tukey's test) (Figure 2). The rank order of potencies was similar at rNa_v1.2a (compound 4>compound 3>compound 6=compound 5=compound 2>>lidocaine), hNa_v1.5 (compound 4>compound 3=compound 6=compound 5=compound 2>>lidocaine) and rNa_v1.8 (compound 4>compound 3>compound 6=compound 5=compound 2>>lidocaine) VGSC subtypes. There were statistically significant differences between the potencies of each dimer for the three respective VGSC subtypes (One-way ANOVA, p< 0.05), however these were small (≤ 10-fold). Thus, lidocaine and compound 2 were significantly less potent at rNa_v1.2a than at both hNa_v1.5 and rNa_v1.8 subtypes whereas compounds 5 and 6 were significantly less potent at rNa_v1.2a than at hNa_v1.5 (p< 0.05, Tukey's test). Compounds 3 and 4 were significantly less potent at both rNa_v1.2a and hNa_v1.5 subtypes than rNa_v1.8 (p<0.05, Tukey's test). Under the present experimental conditions the values for the Hill coefficients for the lidocaine dimers were, in general, greater than 1.0 at all VGSC subtypes. However, there were no consistent differences between the Hill slopes for the dimers and lidocaine.

To probe the specificity of the interaction of the most potent dimer, compound **4**, with VGSCs the effects of three control compounds (compounds **7**, **8** and **9**) (Figure 1) were examined. These compounds comprise of a single lidocaine moiety coupled to a C₄ linker where the second lidocaine moiety has been replaced by one of three functional groups, corresponding to critical components of the local anesthetic pharmacophore, specifically an amine (positively-charged nitrogen), amide and arene group (Rang and Dale, 1991). Compound **7** had no effect on Na⁺ channel activator-evoked depolarization up to a concentration of 100 μ M, the highest concentration tested (Table 1). In contrast, compounds **8** and **9** both inhibited activator-evoked depolarization, but were at least one order of magnitude less potent than compound **4** itself at the respective VGSC subtypes ($p < 0.001$, Tukey's test) (Table 1).

Lidocaine dimers are potent, strongly use-dependent inhibitors of rNa_v1.2a, hNa_v1.5 and rat dorsal root ganglia tetrodotoxin-resistant VGSCs

The inhibitory properties of the dimers at rNa_v1.2a, hNa_v1.5 and rat DRG tetrodotoxin-resistant VGSCs were examined using whole cell voltage-clamp techniques.

The characteristics of hNa_v1.5 Na⁺ current block by lidocaine (300 μ M) and most potent dimer, compound **4** (3 μ M) are illustrated by the representative raw current traces in Figure 3 (Figure 3a and 3c, insets). Lidocaine (300 μ M), inhibited the first and last pulses in the 5 Hz train by 53 ± 0.3 % (tonic inhibition) and 84 ± 0.9 % (phasic inhibition) ($n = 3$ cells), respectively. In contrast, for compound **4** (3 μ M) there was minimal (15 ± 8 %) tonic inhibition, but 80 ± 5 % inhibition of the last pulse of the train (phasic inhibition) ($n = 3$ cells). Concentration-response curves for tonic and phasic block of hNa_v1.5 Na⁺ currents by lidocaine (10 - 300 μ M) and compound **4** (0.1 - 30 μ M) were constructed (Figure 3b, d) and the corresponding pIC₅₀ values calculated (Table 2). Using the present voltage clamp protocols, compound **4** was approximately 60-fold more potent than lidocaine and was

strongly use-dependent, with a 30-fold shift in the potency for phasic block, relative to tonic. Interestingly, the use-dependent component of block reached steady-state rapidly for each concentration of lidocaine tested but for compound **4** true steady-state inhibition was not reached during the 200 pulse train (Figure 3a, c). This most likely reflects the differences in the dissociation rates of the compounds (see below).

The characteristics of inhibition of neonatal rat tetrodotoxin-resistant Na^+ currents (Figure 4), by lidocaine and compound **4**, were very similar to those for inhibition of $\text{hNa}_v1.5$ Na^+ currents. Compound **4** exhibited strong use-dependent inhibition of rat tetrodotoxin-resistant Na^+ currents. At a concentration of $3 \mu\text{M}$ there was minimal ($\sim 5\%$) tonic inhibition, but $84 \pm 4\%$ inhibition of the last pulse of the train (phasic inhibition) ($n = 3$ cells) (see inset Figures 4a, c). The tonic and phasic pIC_{50} values for inhibition of rat tetrodotoxin-resistant Na^+ currents by lidocaine and compound **4** were 3.8 and < 4.5 (tonic) and, 4.1 and 6.3 (phasic), respectively ($n \geq 3$ cells). Similar data were obtained for inhibition of $\text{rNa}_v1.2a$ Na^+ currents by lidocaine and compound **4** (pIC_{50} values = < 3.5 and < 4.5 (tonic) and < 3.5 and 6.0 (phasic), respectively ($n \geq 3$ cells)).

In summary, under the present recording conditions, there was a small (≤ 10 -fold) difference between the tonic potencies of lidocaine and compound **4**, in comparison to a 60- to 300-fold difference between the phasic potencies, at the respective three VGSC subtypes. Compound **4** was strongly use-dependent with a > 30 -fold difference between the tonic and phasic IC_{50} values, in comparison to a < 5 -fold difference for lidocaine. The rank order of potency of compound **4**, for phasic inhibition of VGSC Na^+ currents, was rat dorsal root ganglia tetrodotoxin-resistant $> \text{rNa}_v1.2a = \text{hNa}_v1.5$. However, the absolute difference in potency for inhibition of the three VGSC subtypes was ≤ 2 -fold.

The tonic and phasic pIC_{50} values for compounds **1** to **9** were determined on $\text{hNa}_v1.5$ Na^+ currents (Table 2). There was a reasonable correlation ($r^2=0.6$, slope=0.7, $n=8$) between the phasic and FLIPR pIC_{50} values for these compounds, supporting the conclusion that the

potency of the dimers is dependent upon the length of the tether. Further, the dimers each exhibited use-dependent block with a difference between the tonic and phasic IC_{50} values of approximately 10-fold, or greater. The control compounds, **8** and **9**, were both approximately one order of magnitude less potent than compound **4** for phasic block (Table 2). The kinetics of inhibition of $hNa_v1.5$ Na^+ currents by compound **9** were similar to those of lidocaine such that inhibition of the current reached steady-state during the 200 pulse train (data not shown). In contrast, compound **8** had a profile similar to compound **4**, and steady-state inhibition was not achieved during the 200 pulse train (data not shown). As noted previously, this most likely reflects the differences in dissociation rates of the compounds (see below). Unfortunately, it was not possible to assess the potency of compound **7** using voltage-clamp techniques since at concentrations $> 10 \mu M$ the compound disrupted the established giga-seal.

The rate of dissociation of lidocaine dimers from VGSCs is dependent upon the length of the tether

$hNa_v1.5$ -293-EBNA cells were exposed to equi-effective (approximate phasic IC_{80}) concentrations (in parentheses) of lidocaine (300 μM), compound **2** (30 μM), compound **3** (10 μM), compound **4** (3 μM), compound **5** (10 μM), compound **6** (10 μM), compound **8** (30 μM) or compound **9** (30 μM), and the rates of recovery from inhibition determined as described in Materials and Methods. The effect of lidocaine was rapidly ($\tau < 10$ s) reversible upon washout (Figure 5a). In contrast, the dimers exhibited slower, linker length-dependent dissociation rates with τ values of 133 s, 3000 s, 41 s and 50 s for compounds **2**, **3**, **5** and **6**, respectively (Figure 5a). There was negligible recovery of the $hNa_v1.5$ Na^+ current from inhibition by compound **4** up to 10 min following washout (Figure 5a). It was not possible to investigate longer washout periods because of instability in the recordings at later time

points, and a τ value was not determined. Therefore, the rank order for dissociation from hNa_v1.5 VGSCs was lidocaine>compound **5**=compound **6**>compound **2**>>compound **3**>compound **4**. The dissociation of compound **4** was not enhanced by changing the holding potential to a more negative potential (-140 mV), during the washout period (data not shown). In contrast to compound **4**, dissociation of both the controls, compounds **8** and **9**, could be observed. Thus, compound **9** had a rapid dissociation rate (τ < 10 s) similar to that of lidocaine, whereas compound **8** had a comparatively slower dissociation rate with a τ value of 233 s. rNa_v1.2a-CHO cells also were exposed to equieffective (approximate phasic IC₈₀) concentrations (in parentheses) of compound **2** (300 μ M), compound **3** (3 μ M), compound **4** (3 μ M), compound **5** (30 μ M) or compound **6** (10 μ M) and the rates of recovery determined. For each compound the dissociation rate from rNa_v1.2a was faster than the corresponding rate from hNa_v1.5, however the rank order was similar (Figure 5b). Thus, the dissociation rates for compounds **2**, **5** and **6** were very rapid (τ values of < 10 s) whereas for compounds **3** and **4** the rates were slower with τ values of 197 s and 335 s, respectively.

Monomeric VGSC inhibitors attenuate compound 4-mediated inhibition of hNa_v1.5 VGSCs

To investigate the relationship between the well-characterized local anesthetic binding site and the compound **4** binding site(s) on VGSCs the effect of co-incubation with local anesthetic receptor site inhibitors, or tetrodotoxin, on compound **4**-mediated inhibition of hNa_v1.5 Na⁺ currents was evaluated. hNa_v1.5-293-EBNA cells were incubated with compound **4**, in the absence, or presence, of a local anesthetic or tetrodotoxin, as described in the methods. At the end of the stimulus train the compounds were washed out and current magnitude monitored at a frequency of 0.2 Hz for a further 10 min.

Compound **4** (1 μ M) produced 44 ± 7 % (n= 3 cells) inhibition of hNa_v1.5 Na⁺ currents, which was maintained up to 10 min following washout (Figure 6a, control), consistent with those

data described in the previous section. In contrast, following coincubation with mexiletine (1 mM), but not tetrodotoxin (100 μ M), negligible compound **4**-mediated inhibition was apparent following washout (Figure 6a). Application of mexiletine (1 mM) or tetrodotoxin (100 μ M), alone, produced complete inhibition of hNa_v1.5 Na⁺ currents which recovered to pre-drug amplitudes within 10 s of inhibitor washout (n = 3 cells, data not shown). In subsequent experiments, hNa_v1.5-293-EBNA cells were incubated with increasing concentrations of compound **4**, in the absence, or presence, of a fixed concentration of mexiletine and concentration-response curves of normalized current amplitude (at 10 min following compound washout) constructed. Coincubation with mexiletine (0.3 or 1 mM) produced parallel, rightward shifts in the compound **4** concentration-response curve (Figure 6b). The corresponding Hill coefficients for compound **4** were 1.2, 1.1 and 1.3 in the absence and presence of 0.3 and 1 mM mexiletine, respectively. Similar experiments were conducted using lidocaine (1 mM), bupivacaine (1 mM) and pimozone (0.01 mM) (data not shown). The respective pIC₅₀ values for phasic inhibition were calculated and then, using the Schild equation (Arunlakshana and Schild, 1959), the apparent pK_b values for the different VGSC inhibitors were determined (Table 3). There was a good correspondence between the pK_b values and the respective phasic pIC₅₀ values at hNa_v1.5 (Table 2).

Monomeric VGSC inhibitors increase the rate of dissociation of compound 4 from hNa_v1.5 VGSCs

The observation that coincubation with local anesthetic receptor site inhibitors attenuated interaction of compound **4** with hNa_v1.5 VGSCs is consistent with competitive antagonism. However, a strong negative allosteric interaction between local anesthetic receptor site inhibitors and compound **4** cannot be ruled out. To examine further the relationship between

the compound **4** binding-site(s) and the local anesthetic binding site the influence of free VGSC inhibitors on the dissociation of compound **4** from hNa_v1.5 VGSCs was studied.

hNa_v1.5-293-EBNA cells were incubated with compound **4** (10 μM), as described in the methods, to elicit maximal occupancy of the hNa_v1.5 VGSCs. At the end of the stimulus train compound **4** was washed out and replaced with a monomeric VGSC inhibitor for a specified time ("chase period"), or drug-free extracellular buffer (control). Current magnitude was monitored (at a frequency of 0.2 Hz) throughout the duration of the inhibitor application and, for an additional 5 min washout period, with drug-free extracellular buffer.

Under control conditions, compound **4** (10 μM) produced $94 \pm 2\%$ (n= 3 cells) inhibition of hNa_v1.5 Na⁺ currents, which was maintained up to 10 min following washout of the compound (Figures 7a and 7c, control). However, following chase (5 min) with increasing concentrations of lidocaine, there was a significant increase in the magnitude of the residual Na⁺ current, determined at 5 min after washout of lidocaine (Figure 7a) (One way Anova, $p < 0.0001$; Dunnetts t-test, $p > 0.05$, $p < 0.05$, $p < 0.01$, $p < 0.01$ for 0.3, 1.0, 3.0 and 10 mM lidocaine, respectively). Similar results were obtained with increasing concentrations of mexiletine (Figure 7c) (One-way Anova, $p < 0.0001$; Dunnetts t-test, $p > 0.05$, $p > 0.05$, $p < 0.01$, $p < 0.01$ for 0.1, 0.3, 1.0 and 3.0 mM mexiletine, respectively). Collectively, these data suggest that both lidocaine and mexiletine produced a concentration-dependent increase in the rate of dissociation of compound **4** from hNa_v1.5 VGSCs. Consistent with the hypothesis that monomeric inhibitors increased the rate of dissociation of compound **4**, a time-dependent increase in the magnitude of the residual Na⁺ current (determined at 5 min after washout of the inhibitor) was observed following chase (1, 5 or 10 min) with a fixed concentration of lidocaine (3 mM) or mexiletine (10 mM) (Figures 7b and 7d).

Alternate local anesthetic (bupivacaine) or anticonvulsant (lamotrigine, 4030W92) VGSC inhibitors also accelerated the dissociation of compound **4**. Thus, following a 5 min chase

with a 1 mM concentration of the respective inhibitors, and a subsequent 5 min washout period, at least 40 % recovery of the hNa_v1.5 Na⁺ currents was observed (Table 4). In contrast, the pore-blocking toxin, tetrodotoxin (100 μM) had no significant effect on compound **4** dissociation ($p > 0.38$, unpaired student's *t* test). There was a poor correlation between the tonic and phasic potency values of the inhibitors and their ability to accelerate dissociation of compound **4** (Table 4). Thus, at a concentration of 1 mM, 4030W92 promoted the greatest degree of recovery (67 ± 5 %, $n = 3$) of hNa_v1.5 Na⁺ currents, although this compound exhibited the lowest tonic and phasic potency values (Table 4).

Similar experiments, conducted using rNa_v1.2a-CHO cells, demonstrated that mexiletine also accelerated the dissociation of compound **4** from rNa_v1.2a VGSCs. As described above, in contrast to hNa_v1.5, dissociation of compound **4** from rNa_v1.2a could be observed in the absence of an inhibitor. Thus, under control conditions, at 10 min following washout of compound **4** (10 μM), the residual current was 77 ± 6 % ($n = 3$ cells) of the initial current amplitude. In contrast, following a 5 min chase with 1 mM mexiletine, and a subsequent 5 min washout period, there was a significant increase in the residual current (112 ± 7 %, $n = 3$ cells; $p = 0.02$, unpaired *t*-Test).

Discussion

The present study has demonstrated that N-linked lidocaine dimers, in which the lidocaine moieties are linked by an unsubstituted alkylene chain are potent, use-dependent inhibitors of rNa_v1.2a, hNa_v1.5 and rNa_v1.8 VGSCs. The potency and dissociation rate of the dimers was dependent upon the length of the linker coupling the two lidocaine moieties. The *n*-butylene-linked dimer (compound **4**) was the most potent and exhibited the slowest dissociation rate.

The observation that varying the length of the linker modulated both the potency and dissociation rate of the dimers is consistent with a multivalent interaction at VGSCs (Mammen et al., 1998; Kiessling et al., 2000; Wright and Usher, 2001). A linker length-dependent increase in potency of dimeric ligands, relative to the monomer, has been reported for compounds interacting with cyclic nucleotide-gated (Kramer and Karpen, 1998), SK_{Ca} (Galanakis et al., 1996) and nAChR (Rosini et al., 1999) channels. Polymer-linked cGMP dimers simultaneously occupy two binding sites on the cyclic nucleotide gated channel. Both the potency and dissociation rate of these dimers is dependent upon the length of the linker joining the two cGMP moieties, similar to the present findings. However, in contrast to cyclic nucleotide-gated channels, which are homotetramers with a cGMP binding site on each subunit, the presence of two, or more, distinct binding sites for local anesthetics on VGSCs has yet to be confirmed.

Additional support for a multivalent interaction comes from studies using control compounds. Thus, compound **7**, which retains the amine, but lacks the amide and arene motifs of the second lidocaine moiety had low affinity (pIC₅₀ < 4) for VGSCs. Further, compound **8**, which retains the amine and amide but lacks the arene motif, and compound **9**, which retains the arene but lacks the corresponding amine motif, although more potent VGSC inhibitors than lidocaine, were at least ten-fold less potent than compound **4** and exhibited significantly faster dissociation rates. These data suggest that the presence of a second, intact local

anesthetic pharmacophore was critical to manifest the dramatic increase in potency (relative to lidocaine) and slow dissociation rate of compound **4**.

It is well established that there is a correlation between hydrophobicity and the *in vitro*, and *in vivo*, efficacy of VGSC blockers (Strichartz et al., 1990). However, in the present study the most hydrophobic molecules i.e. compounds **5** and **6** (the relative increase in logD value being ~ 0.5 per methylene unit) had lower *in vitro* potencies and exhibited significantly faster dissociation rates from VGSCs than compounds **3** or **4**. Differences in local anesthetic pK_a values, and hence the relative proportions of cationic and uncharged free amine forms, also can influence the extent and/or kinetics of inhibition of VGSCs (Chernoff and Strichartz, 1990). The calculated pK_a value (Pallas, CompuDrug Intl.) for lidocaine is 8.03. In comparison, for the dimers the calculated pK_a values for the amine in the first lidocaine moiety range from 6.83 (compound **2**) to 8.23 (compounds **5** and **6**) and from 3.79 (compound **2**) to 7.62 (compounds **5** and **6**) in the second moiety. Therefore, it is possible that, with the exception of compounds **5** and **6** which are diprotonated, all the dimers exist as monoprotonated, or even uncharged (i.e. compound **2**) species at physiological pH. The observation that compound **8**, which has very similar calculated pK_a values (7.09, 6.67) to compound **4** (7.37, 6.37), yet exhibited lower potency and a more rapid dissociation rate, is consistent with the proposal that differences in charge state alone are unlikely to account for the dramatic increase in potency and/or kinetic properties of compound **4**. To summarize, it is proposed that the specific structure of compound **4** (as discussed above), and not simply its physical properties (i.e. hydrophobicity, charge state), accounts for the slow dissociation rate and enhanced potency at VGSCs.

The strongest evidence for a bivalent interaction of a lidocaine dimer with VGSCs derives from the observation that free local anesthetics increase the dissociation of compound **4** from hNa_v1.5 and rNa_v1.2a. In monovalent binding, the dissociation of a ligand from its binding site is determined by the rate constant for dissociation and is unaffected by the concentration of a

competing free ligand in solution. However, in bivalent binding, dissociation occurs in stages, and its rate can be accelerated by occupancy of either site by monovalent ligand (Figure 8; Kramer and Karpen, 1998). One interpretation of the present findings is that compound **4** binds to the conserved local anesthetic receptor and a second site. The binding of compound **4** to hNa_v1.5 VGSCs was inhibited, in an apparently competitive manner, by coincubation with local anesthetic, anticonvulsant or antiarrhythmic agents, with estimated pK_b values similar to their corresponding phasic pIC₅₀ values. These data are consistent with the hypothesis that one of the binding sites for compound **4** is the conserved local anesthetic receptor. Free monovalent local anesthetics could accelerate dissociation of compound **4** through occupancy of this site. However, the apparent lack of correlation between the ability of such ligands to enhance the dissociation rate of compound **4** and their affinities for the conserved local anesthetic site suggests instead that these monovalent ligands have some affinity for the second site, and it is through interaction at this site that they promote dissociation of compound **4** (c.f. Figure 8).

The lidocaine dimers may span adjacent domains in the VGSC or, alternatively, bind to vicinal binding sites in the protein, as has been proposed for dequalinium binding to SK_{Ca} channels (Galanakis et al., 1996). A low resolution (19 Å) three-dimensional structure of the VGSC has revealed a pseudotetrameric arrangement of the channel (Sato et al., 2001). Furthermore, as discussed previously, various amino acid residues in transmembrane region S6 from domains 1, 3 and 4 have been shown to be important for local anesthetic binding to VGSCs. However, it is believed that this reflects a domain interface binding site, in which individual amino acid residues from the different S6 regions make binding interactions with the inhibitor, rather than the presence of independent binding sites (Catterall, 2002). Nevertheless, several groups have suggested the presence of additional binding sites for local anesthetics on VGSCs. The presence of two binding sites was proposed as one explanation for the influence of Na⁺ channel activators on stereoselective inhibition by

bupivacaine and other local anesthetics (Lee-Son et al., 1992). More recently, the presence of one, or more, additional binding sites, which are unmasked upon channel activation, has been proposed for both lidocaine (Leuwer et al., 2004) and prenylamine (Mujtaba et al., 2001). Indeed, voltage-clamp and site-directed mutagenesis techniques suggest that prenylamine and bupivacaine act at separate pharmacological receptors on hNa_v1.5 (Mujtaba et al., 2002). Finally, interactions between lidocaine and structural regions of hNa_v1.5 (Bennett et al., 1995) or rNa_v1.2a (Kuroda et al., 1996, 2000) which are responsible for inactivation have been reported.

The present findings of a small (≤ 10 -fold) difference between the tonic potencies of lidocaine and compound **4**, in comparison to the dramatic (60- to 300-fold) difference between the phasic potencies, suggests conformational changes in VGSCs, upon depolarization, expose an additional binding site and/or binding interaction(s) for the second lidocaine moiety and it is the resultant multivalent interaction that underlies the enhanced phasic potency and slow dissociation rate of compound **4**.

One advantage of multivalent ligands is that, in addition to an increase in potency, such compounds may exhibit increased selectivity, as a result of bridging between proximal binding sites which have alternate structure and/or spatial localization on target proteins (Wright and Usher, 2001). In the present study, although the dimers exhibited significant increases in potency, relative to lidocaine, they did not exhibit significant subtype selectivity, suggesting that the identity, orientation and/or distance between the relevant binding sites must be similar for the three VGSCs. This may not be surprising since the nine sodium channel isoforms (Na_v1.1 - Na_v1.9) are greater than 50% identical in amino acid sequence in the extracellular and transmembrane domains (Goldin et al., 2000). Furthermore, in the putative local anesthetic binding site in D4S6 the critical phenylalanine and tyrosine residues (Catterall, 2002) are conserved between Na_v1.2a, Na_v1.5 and Na_v1.8. However, there were

significant differences in the rates of dissociation of the dimers from rNa_v1.2a and hNa_v1.5, which may reflect subtle differences in the interaction with these channels.

In summary, these studies have demonstrated that *N*-linked lidocaine dimers, tethered by unsubstituted alkylene linkers of varying length, are potent, use-dependent VGSC inhibitors. Both the potency and dissociation rate of the dimers was dependent upon the length of the linker coupling the two lidocaine moieties, consistent with a multivalent interaction. Furthermore, the present data suggest that a four carbon alkylene chain provides the optimal three-dimensional orientation for binding within the series, with both lidocaine moieties in compound **4** making specific contacts with the VGSC. The observation that monomeric VGSC inhibitors accelerate the dissociation of compound **4** supports the hypothesis that compound **4** simultaneously occupies two binding sites on VGSCs. Both sites can be bound by local anesthetic, anticonvulsant or antiarrhythmic agents, one being the conventional local anesthetic site and the other an, as yet, undefined site.

Acknowledgements

The authors would like to thank Mathai Mammen for helpful discussion during the preparation of this manuscript.

References

Arunlakshana O and Schild HO (1959) Some Quantitative Uses of Drug Antagonists. *Br J Pharmacol* **14**: 48-58.

Bean BP, Cohen CJ and Tsien RW (1983) Lidocaine Block of Cardiac Sodium Channels. *J Gen Physiol* **81**: 613-642.

Bennett PB, Valenzuela C, Chen LQ and Kallen RG (1995) On the Molecular Nature of the Lidocaine Receptor of Cardiac Na⁺ Channels. Modification of Block by Alterations in the Alpha-Subunit III-IV Interdomain. *Circ Res* **77**: 584-592.

Catterall WA (2000) From Ionic Currents to Molecular Mechanisms: the Structure and Function of Voltage-Gated Sodium Channels. *Neuron* **26**: 13-25.

Catterall WA (2002) Molecular Mechanisms of Gating and Drug Block of Sodium Channels. *Novartis Found Symp* **241**:206-218.

Cestele S and Catterall WA (2000) Molecular mechanisms of neurotoxin action on voltage-gated sodium channels. *Biochimie* **82**:883-92.

Chernoff DM and Strichartz GR (1990) Kinetics of Local Anesthetic Inhibition of Neuronal Sodium Currents. PH and Hydrophobicity Dependence. *Biophys J* **58**: 69-81.

Christopoulos A, Grant MK, Ayoubzadeh N, Kim ON, Sauerberg P, Jeppesen L, El-Fakahany EE (2001) Synthesis and pharmacological evaluation of dimeric muscarinic acetylcholine receptor agonists. *J Pharmacol Exp Ther* **298**:1260-8.

Galanakis D, Ganellin CR, Dunn PM and Jenkinson DH (1996) On the Concept of a Bivalent Pharmacophore for SKCa Channel Blockers: Synthesis, Pharmacological Testing, and

Radioligand Binding Studies on Mono-, Bis-, and Tris-Quinolinium Compounds. *Arch Pharm (Weinheim)* **329**: 524-528.

Goldin AL, Barchi RL, Caldwell JH, Hofmann F, Howe JR, Hunter JC, Kallen RG, Mandel G, Meisler MH, Netter YB, Noda M, Tamkun MM, Waxman SG, Wood JN and Catterall WA (2000) Nomenclature of Voltage-Gated Sodium Channels. *Neuron* **28**: 365-368.

Halazy S, Perez M, Fourrier C, Pallard I, Pauwels PJ, Palmier C, John GW, Valentin JP, Bonnafous R and Martinez J (1996) Serotonin Dimers: Application of the Bivalent Ligand Approach to the Design of New Potent and Selective 5-HT(1B/1D) Agonists. *J Med Chem* **39**: 4920-4927.

Hille B (2001) in *Ion Channels of Excitable Membranes*, Sinauer Associates, Sunderland, MA.

Hockerman GH, Johnson BD, Abbott MR, Scheuer T, Catterall WA (1997) Molecular determinants of high affinity phenylalkylamine block of L-type calcium channels in transmembrane segment IIIS6 and the pore region of the alpha1 subunit. *J Biol Chem* **272**:18759-65.

Hondeghem LM and Katzung BG (1977) Time- and Voltage-Dependent Interactions of Antiarrhythmic Drugs With Cardiac Sodium Channels. *Biochimica et Biophysica Acta* **472**: 373-398.

Joslyn AF, Luchowski E and Triggle DJ (1988) Dimeric 1,4-Dihydropyridines As Calcium Channel Antagonists. *J Med Chem* **31**: 1489-1492.

Kiessling LL, Strong L E and Gestwicki JE (2000) Principles for Multivalent Ligand Design. *Annual Reports in Medicinal Chemistry* **35**, 321-330.

Kizuka H and Hanson RN (1987) Beta-adrenoceptor antagonist activity of bivalent ligands. 1. Diamide analogues of practolol. *J Med Chem* **30**:722-6.

Kramer RH and Karpen JW (1998) Spanning Binding Sites on Allosteric Proteins With Polymer-Linked Ligand Dimers. *Nature* **395**: 710-713.

Kuroda Y, Ogawa M, Nasu H, Terashima M, Kasahara M, Kiyama Y, Wakita M, Fujiwara Y, Fujii N and Nakagawa T (1996) Locations of Local Anesthetic Dibucaine in Model Membranes and the Interaction Between Dibucaine and a Na⁺ Channel Inactivation Gate Peptide As Studied by 2H- and 1H-NMR Spectroscopies. *Biophys J* **71**: 1191-1207.

Kuroda Y, Miyamoto K, Tanaka K, Maeda Y, Ishikawa J, Hinata R, Otaka A, Fujii N and Nakagawa T (2000) Interactions Between Local Anesthetics and Na⁺ Channel Inactivation Gate Peptides in Phosphatidylserine Suspensions As Studied by 1H-NMR Spectroscopy. *Chem Pharm Bull (Tokyo)* **48**: 1293-1298.

Leboulluec KL, Mattson R J, Mahle C D, McGovern R T, Nowak H P and Gentile A J (1995) Bivalent Indoles Exhibiting Serotonergic Binding Affinity. *Bioorganic & Medicinal Chemistry Letters* **5**: 123-126.

Lee-Son S, Wang G K, Concus A, Crill E and Strichartz G (1992) Stereoselective Inhibition of Neuronal Sodium Channels by Local Anesthetics. Evidence for Two Sites of Action? *Anesthesiology* **77**: 324-335.

Leuwer M, Haeseler G, Hecker H, Bufler J, Dengler R and Aronson J K (2004) An Improved Model for the Binding of Lidocaine and Structurally Related Local Anaesthetics to Fast-Inactivated Voltage-Operated Sodium Channels, Showing Evidence of Cooperativity. *Br J Pharmacol* **141**: 47-54.

Mammen M, Choi S-K and Whitesides GM (1998) Polyvalent Interactions in Biological Systems: Implications for Design and Use of Multivalent Ligands and Inhibitors. *Angew Chem Int Ed Engl* **37**: 2754-2794.

Mujtaba MG, Gerner P and Wang G K (2001) Local Anesthetic Properties of Prenylamine. *Anesthesiology* **95**: 1198-1204.

Mujtaba MG, Wang SY, Wang GK (2002) Prenylamine block of Nav1.5 channel is mediated via a receptor distinct from that of local anesthetics. *Mol Pharmacol* **62**:415-22.

Nau C, Wang S Y, Strichartz G R and Wang G K (1999) Point Mutations at N434 in D1-S6 of Mu1 Na(+) Channels Modulate Binding Affinity and Stereoselectivity of Local Anesthetic Enantiomers. *Mol Pharmacol* **56**: 404-413.

Portoghese PS, Nagase H, Lipkowski AW, Larson DL and Takemori AE (1988) Binaltorphimine-Related Bivalent Ligands and Their Kappa Opioid Receptor Antagonist Selectivity. *J Med Chem* **31**: 836-841.

Ragsdale DS, Scheuer T and Catterall WA (1991) Frequency and Voltage-Dependent Inhibition of Type IIA Na⁺ Channels, Expressed in a Mammalian Cell Line, by Local Anesthetic, Antiarrhythmic, and Anticonvulsant Drugs. *Mol Pharmacol* **40**: 756-765.

Ragsdale DS, McPhee J C, Scheuer T and Catterall W A (1996) Common Molecular Determinants of Local Anesthetic, Antiarrhythmic, and Anticonvulsant Block of Voltage-Gated Na⁺ Channels. *Proc Natl Acad Sci U S A* **93**: 9270-9275.

Rang HP and Dale M (1991) in *Pharmacology*. Churchill Livingstone

Rosini M, Budriesi R, Bixel MG, Bolognesi ML, Chiarini A, Hucho F, Krosgaard-Larsen P, Mellor IR, Minarini A, Tumiatti V, Usherwood PN, Melchiorre C (1999) Design, synthesis, and

biological evaluation of symmetrically and unsymmetrically substituted methoctramine-related polyamines as muscular nicotinic receptor noncompetitive antagonists. *J Med Chem* **42**:5212-23.

Sato C, Ueno Y, Asai K, Takahashi K, Sato M, Engel A, Fujiyoshi Y (2001) The voltage-sensitive sodium channel is a bell-shaped molecule with several cavities *Nature* **409**: 1047-51.

Strichartz GR, Sanchez V, Arthur GR, Chafetz R and Martin D (1990) Fundamental Properties of Local Anesthetics. II. Measured Octanol:Buffer Partition Coefficients and PKa Values of Clinically Used Drugs. *Anesth Analg* **71**:158-170.

Vickery RG, Amagasu SM, Chang R, Mai N, Kaufman E, Martin J, Hembrador J, O'Keefe M D, Gee C, Marquess D and Smith JA (2004) Comparison of the Pharmacological Properties of Rat Na(V)1.8 With Rat Na(V)1.2a and Human Na(V)1.5 Voltage-Gated Sodium Channel Subtypes Using a Membrane Potential Sensitive Dye and FLIPR. *Receptors Channels* **10**: 11-23.

Wang SY, Nau C and Wang G K (2000) Residues in Na(+) Channel D3-S6 Segment Modulate Both Batrachotoxin and Local Anesthetic Affinities. *Biophys J* **79**: 1379-1387.

Weiser T, Qu Y, Catterall WA and Scheuer T (1999) Differential Interaction of R-Mexiletine With the Local Anesthetic Receptor Site on Brain and Heart Sodium Channel Alpha-Subunits. *Mol Pharmacol* **56**: 1238-1244.

Wright D and Usher L (2001) Multivalent Binding in the Design of Bioactive Compounds. *Current Organic Chemistry* **5**: 1107-1131.

Yarov-Yarovoy V, Brown J, Sharp EM, Clare JJ, Scheuer T and Catterall WA (2001)
Molecular Determinants of Voltage-Dependent Gating and Binding of Pore-Blocking Drugs in
Transmembrane Segment IIIS6 of the Na(+) Channel Alpha Subunit. *J Biol Chem* **276**: 20-
27.

Yarov-Yarovoy V, McPhee JC, Idsvoog D, Pate C, Scheuer T and Catterall WA (2002) Role
of Amino Acid Residues in Transmembrane Segments IS6 and IIS6 of the Na⁺ Channel
Alpha Subunit in Voltage-Dependent Gating and Drug Block. *J Biol Chem* **277**: 35393-35401.

Footnotes

For reprints contact:

Jacqueline Smith

Theravance Inc.,

901 Gateway Blvd.,

South San Francisco CA 94080

Tel: 650-808-6415

Fax: 650-808-6886

E-mail: jsmith@theravance.com

¹Current address: Pharmacofore, Inc., 1070 Arastradero Road, Suite 300, Palo Alto, CA 94304, USA

Legends for Figures

Figure 1. Structures of lidocaine (compound **1**), symmetrical, *N*-linked lidocaine dimers, tethered by an unsubstituted alkylene linker ($n = 2$ to 6 methylene units; compounds **2-6**) and three control molecules (compounds **7**, **8**, **9**).

Figure 2. Effect of lidocaine and compounds **2** to **6** on Na^+ channel activator-evoked depolarization of $\text{rNa}_v1.2\text{a-CHO}$ (hatched bars), $\text{hNa}_v1.5\text{-293-EBNA}$ (gray bars) and $\text{rNa}_v1.8\text{-F-11}$ (solid bars) cells. FMP dye-loaded cells were incubated for 30 min in the absence, or presence, of antagonist. Membrane potential then was monitored using a FLIPR^R before, and after, the addition of veratridine (20 μM); veratridine (20 μM) plus deltamethrin (3 μM) or veratridine (20 μM) plus deltamethrin (20 μM), respectively, to elicit membrane depolarization. Data represents mean \pm s.d. of 4-26 independent pIC_{50} determinations, each performed in duplicate. *** $p < 0.001$ and ** $p < 0.01$, significantly different from $\text{rNa}_v1.8$; †† $p < 0.01$ and † $p < 0.05$, significantly different from $\text{hNa}_v1.5$ and ‡‡ $p < 0.01$, significantly different from both $\text{hNa}_v1.5$ and $\text{rNa}_v1.8$ (Tukey's multiple comparison test).

Figure 3. Tonic and phasic inhibition of $\text{hNa}_v1.5$ Na^+ currents by lidocaine and compound **4**. Normalized current responses in the presence of increasing concentrations of a) lidocaine (closed triangles, 10 μM ; open triangles, 30 μM ; closed squares, 100 μM ; open squares, 300 μM) and c) compound **4** (closed triangles, 0.1 μM ; open triangles, 0.3 μM ; closed squares, 1 μM ; open squares, 3 μM ; closed circles, 10 μM ; open circles, 30 μM). Na^+ current magnitude was monitored, at a frequency of 0.2 Hz, for a period of one min. Cells then were exposed to lidocaine or compound **4** in the absence of depolarizing pulses for 3 min, followed by a 5 Hz train of 200 pulses (10 ms duration) from the holding potential (-120 mV) to the test potential (-20 mV), in the continuous presence of compound. Current amplitudes were normalized to

the initial current in the absence of compound. Insets: Representative current traces evoked by a single pulse in the absence of compound (control) and by pulses 1 and 200 of the train, in the presence of 300 μ M lidocaine (inset a) or 3 μ M compound **4** (cpd **4**, inset c). Concentration-response curves showing effect of b) lidocaine and d) compound **4**, on the amplitude of the first (closed squares) and last (open squares) depolarizations in the 200 pulse train. Data represents mean \pm s.e.mean of at least 3 cells. In panels a and c the standard error bars have been omitted for clarity.

Figure 4. Tonic and phasic inhibition of rat tetrodotoxin-resistant Na⁺ currents by lidocaine and compound **4**. Normalized current responses in the presence of increasing concentrations of a) lidocaine (closed triangles, 10 μ M; open triangles, 30 μ M; closed squares, 100 μ M; open squares, 300 μ M) and c) compound **4** (closed triangles, 0.1 μ M; open triangles, 0.3 μ M; closed squares, 1 μ M; open squares, 3 μ M; closed circles, 10 μ M; open circles, 30 μ M). Na⁺ current magnitude was monitored, at a frequency of 0.2 Hz, for a period of one min. Cells then were exposed to lidocaine or compound **4** in the absence of depolarizing pulses for 3 min, followed by a 5 Hz train of 200 pulses (10 ms duration) from the holding potential (-90 mV) to the test potential (-0 mV), in the continuous presence of compound. Current amplitudes were normalized to the initial current in the absence of compound and then corrected for current run down, as described in the methods section. Insets: Representative current traces evoked by a single pulse in the absence of compound (control) and by pulses 1 and 200 of the train, in the presence of 300 μ M lidocaine (inset a) or 3 μ M compound **4** (cpd **4**, inset c). Concentration-response curves showing effect of b) lidocaine and d) compound **4**, on the amplitude of the first (closed squares) and last (open squares) depolarizations in the 200 pulse train. Data represents mean \pm s.e.mean of at least 3 cells. In panels a and c the standard error bars have been omitted for clarity.

Figure 5. Dissociation of lidocaine and lidocaine dimers from hNa_v1.5 and rNa_v1.2a VGSCs. hNa_v1.5-293-EBNA cells (a) and rNa_v1.2a-CHO cells (b) were exposed to lidocaine or dimer, in the absence of depolarizing pulses for 3 min, followed by a 5 Hz train of 200 pulses (10 ms duration), in the continuous presence of the compound. At the end of the train the compound was washed out and current magnitude monitored at a frequency of 0.2 Hz for 10 min, as described in the methods. Compounds were applied for the period indicated by the black bar. hNa_v1.5-293-EBNA cells were exposed to approximate phasic IC₈₀ concentrations: lidocaine (closed triangles, 300 μM), compound **2** (open triangles, 30 μM), compound **3** (closed squares, 10 μM), compound **4** (open squares, 3 μM), compound **5** (closed circles, 10 μM) or compound **6** (open circles, 10 μM) dimer. rNa_v1.2a-CHO cells were exposed to concentrations which corresponded to the approximate phasic IC₈₀ values for inhibition of hNa_v1.5 Na⁺ currents: compound **2** (open triangles, 300 μM), compound **3** (closed squares, 3 μM), compound **4** (open squares, 3 μM), compound **5** (closed circles, 30 μM) or compound **6** (open circles, 10 μM) dimer. Current amplitudes were normalized to the initial current in the absence of compound. Data represents mean ± s.e.mean of at least 3 cells. In panels a and b, for the purposes of clarity, only every 3rd data point is shown.

Figure 6. Effect of mexiletine or tetrodotoxin on compound **4**-mediated inhibition of hNa_v1.5 Na⁺ currents. In a) hNa_v1.5-293-EBNA cells were incubated with compound **4** (1 μM), in the absence (control, closed squares), or presence, of mexiletine (open triangles, 1 mM) or tetrodotoxin (tetrodotoxin; open circles, 100 μM), according to the protocol described in the methods. At the end of the stimulus train the compounds were washed out and current magnitude monitored at a frequency of 0.2 Hz for a further 10 min. Compounds were applied for the period indicated by the black bar. b) Concentration-response curves showing effect of

compound **4**, in the absence (closed squares) or presence of mexiletine (closed triangles, 300 μ M; open triangles, 1 mM), on the amplitude of the last depolarization i.e. 10 min following drug washout. Data represents mean \pm s.e.mean of at least 3 cells.

Figure 7. Effect of free VGSC inhibitor on the dissociation of compound **4** from hNa_v1.5 VGSCs. hNa_v1.5-293-EBNA cells were incubated with compound **4** (10 μ M), according to the standard protocol described in the methods, to elicit full occupancy of the hNa_v1.5 VGSCs. At the end of the stimulus train compound **4** was washed out and replaced with extracellular buffer (closed triangles, control) or inhibitor (lidocaine or mexiletine) for a specified time ("chase period"). In a) and c) cells were incubated with increasing concentrations of a) lidocaine (open triangles, 0.3 mM; closed squares, 1.0 mM; open squares, 3.0 mM; closed circles, 10 mM) or c) mexiletine (open triangles, 0.1 mM; closed squares, 0.3 mM; open squares, 1.0 mM; closed circles, 3.0 mM) for a 5 min chase period. In b) lidocaine (3.0 mM) or d) mexiletine (1.0 mM) were applied for 1 (closed triangles), 5 (open triangles) or 10 (open squares) min chase periods. Current magnitude was monitored (at a frequency of 0.2 Hz) throughout the duration of the inhibitor application and an additional 5 min washout period, with drug-free extracellular buffer. Compounds were applied for the period(s) indicated by the black bar. Data represents mean \pm s.e.mean of at least 3 cells.

Figure 8. Schematic representation of a putative model for interaction of lidocaine dimers with VGSCs. The lidocaine dimer simultaneously occupies two proximal binding sites on the VGSC, one of which is the conventional local anesthetic site (denoted "LA site", semicircular) and the second an, as yet, undefined site (rectangular). When one of the lidocaine moieties in the dimer dissociates it has a high probability of rebinding before its partner can also dissociate. This results in a decrease in the dissociation rate of the dimer. Occupancy of the

binding site with competing ligand i.e. free local anesthetic (or alternate VGSC inhibitor), prevents this rebinding event and hence speeds the dissociation of the dimer. For the purposes of clarity, only those interactions which are most relevant to the hypothetical model are shown. Therefore, interaction of free local anesthetic at the “LA site” is not shown, given the poor correlation between the tonic and phasic potency values of local anesthetic ligands and their ability to accelerate dissociation of the dimer.

Tables

Table I. pIC₅₀ values for lidocaine and lidocaine dimers at rNa_v1.2a, hNa_v1.5 and rNa_v1.8 recombinant VGSCs determined using FLIPR^R membrane potential assay.

	rNa _v 1.2a	n	hNa _v 1.5	n	rNa _v 1.8	n
	pIC ₅₀		pIC ₅₀		pIC ₅₀	
Lidocaine	3.7 ± 0.2	21	4.1 ± 0.1	26	4.1 ± 0.2	23
Compound 2	4.7 ± 0.2	7	5.7 ± 0.1	4	5.4 ± 0.1	4
Compound 3	5.4 ± 0.2	8	5.5 ± 0.2	4	6.2 ± 0.3	4
Compound 4	6.0 ± 0.4	15	6.2 ± 0.2	11	6.8 ± 0.1	9
Compound 5	5.0 ± 0.2	9	5.4 ± 0.3	6	5.2 ± 0.1	4
Compound 6	5.0 ± 0.3	5	5.5 ± 0.1	4	5.1 ± 0.2	4
Compound 7	<4	4	<4	4	3.5 ± 0.2	4
Compound 8	<4	4	4.7 ± 0.4	4	4.7 ± 0.1	4
Compound 9	5.0 ± 0.2	4	4.9 ± 0.2	4	5.3 ± 0.1	4
TTX	8.7 ± 0.2	4	5.6 ± 0.2	22	< 4.0	8

Data represents mean ± s.d. of number of observations (n) indicated.

Activation of Na⁺ channels in FMP-dye loaded rNa_v1.2a-CHO, hNa_v1.5-293-EBNA and rNa_v1.8-F-11 cells was achieved using veratridine (20 μM); veratridine (20 μM) plus deltamethrin (3 μM) and veratridine (20 μM) plus deltamethrin (20 μM), respectively.

Table 2. Tonic and phasic Inhibition of hNa_v1.5 Na⁺ currents by lidocaine and lidocaine dimers determined using whole cell voltage-clamp.

	hNa _v 1.5 Tonic pIC ₅₀	hNa _v 1.5 Phasic pIC ₅₀
Lidocaine	3.5	4.2
Compound 2	3.9	4.9
Compound 3	4.2	5. 4
Compound 4	4.5	6.0
Compound 5	4.6	5.8
Compound 6	4.9	5.8
Compound 7	*	*
Compound 8	3.9	4.9
Compound 9	3.8	5.1

Data represents mean of 3 cells. n.d., not determined.

* compound inhibited formation of gigaseal at 10 μM.

Table 3. Antagonism of Compound **4** mediated inhibition of hNa_v1.5 Na⁺ Currents by VGSC Inhibitors.

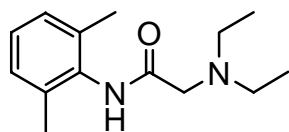
VGSC Inhibitor	hNa _v 1.5 Apparent pK _b	hNa _v 1.5 Phasic pIC ₅₀
Lidocaine	4.3	4.2
Mexiletine		
1 mM	4.1	4.3
0.3 mM	4.3	
Bupivacaine	4.8	5.0
Pimozide	6.4	5.6

Cells were coincubated with increasing concentrations of compound **4** in the absence, or presence, of a fixed concentration of lidocaine (1 mM), mexiletine (0.3 or 1 mM), bupivacaine (1 mM) or pimozide (10 μM), and the standard protocol (described in the methods) applied. The extent of residual inhibition was determined at 10 min following washout of both compounds. Compound **4** concentration response curves (mean of $n \geq 3$ cells per concentration) were constructed and pK_b values for the VGSC inhibitors were determined using the Schild Equation (Arunlakshana and Schild, 1959).

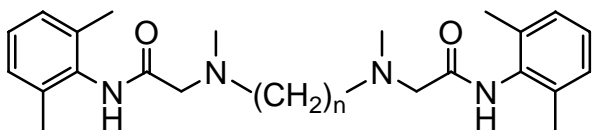
Table 4. Effect of free LA, antiarrhythmic or anticonvulsant VGSC inhibitors on the dissociation of Compound **4** from hNa_v1.5 VGSCs.

VGSC Inhibitor	hNa _v 1.5 Tonic IC ₅₀ (μM)	hNa _v 1.5 Phasic IC ₅₀ (μM)	Chase Conc. (mM)	% Recovery of Na ⁺ current
Control	n/a	n/a	n/a	6 ± 2
Lidocaine	292	57	3	46 ± 5
Mexiletine	168	59	1	49 ± 9
Bupivacaine	94	12	1	53 ± 2
Lamotrigine	185	144	1	40 ± 3
4030W92	>300	296	1	67 ± 5

hNa_v1.5-293-EBNA cells were incubated with compound **4** (10 μM), as described in the methods, to elicit full occupancy of the hNa_v1.5 VGSCs. At the end of the stimulus train compound **4** was washed out and replaced with VGSC inhibitor (at the concentrations specified), or drug-free extracellular buffer (control), for a 5 minute “chase period”. Current magnitude was monitored (at a frequency of 0.2 Hz) throughout the duration of the inhibitor application and for an additional 5 min washout period, with drug-free extracellular buffer. The extent of recovery of the hNa_v1.5 Na⁺ current, relative to the initial current amplitude, was determined at the end of the 5 min washout. Tonic and phasic IC₅₀ values, for the various VGSC inhibitors, were determined using the standard protocol, described in the methods (n ≥ 3 cells). % Recovery data represents mean ± sem (n ≥ 3 cells).



lidocaine (compound 1)



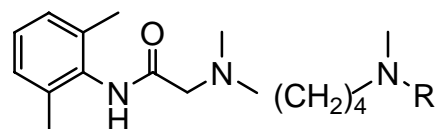
compound 2: $n=2$

compound 3: $n=3$

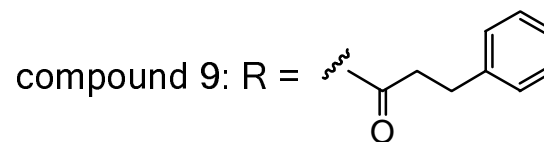
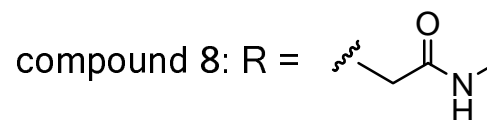
compound 4: $n=4$ (THR-170148)

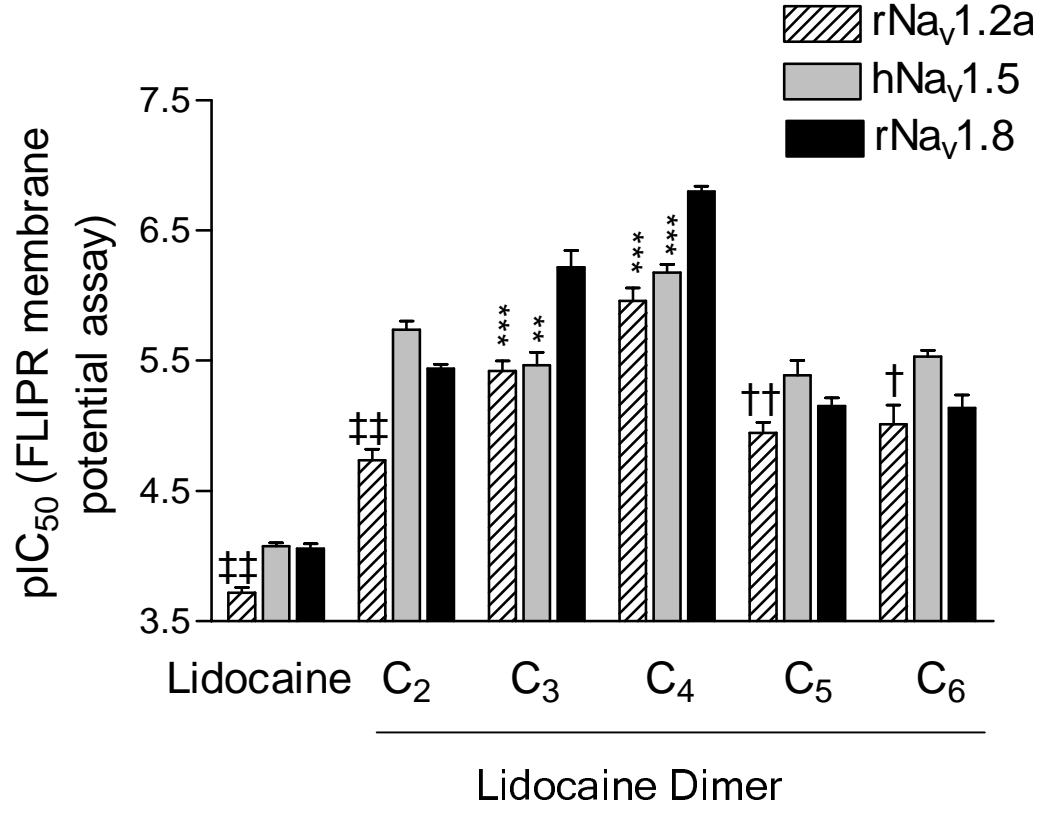
compound 5: $n=5$

compound 6: $n=6$

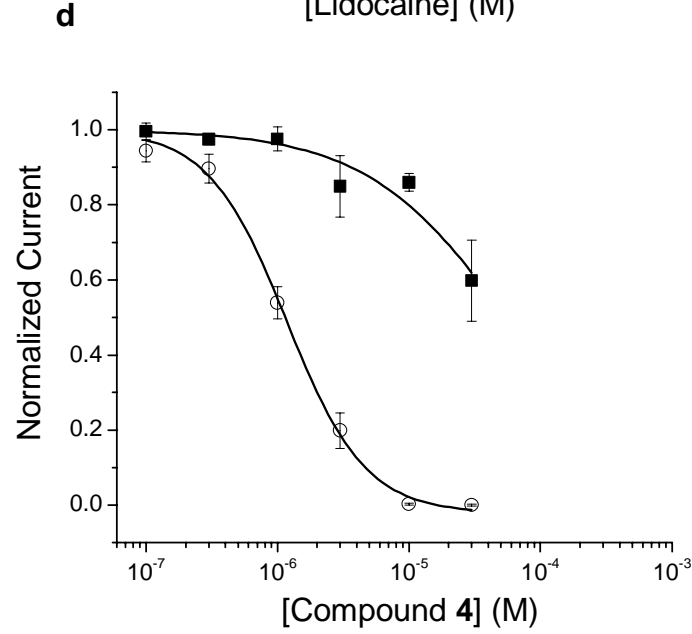
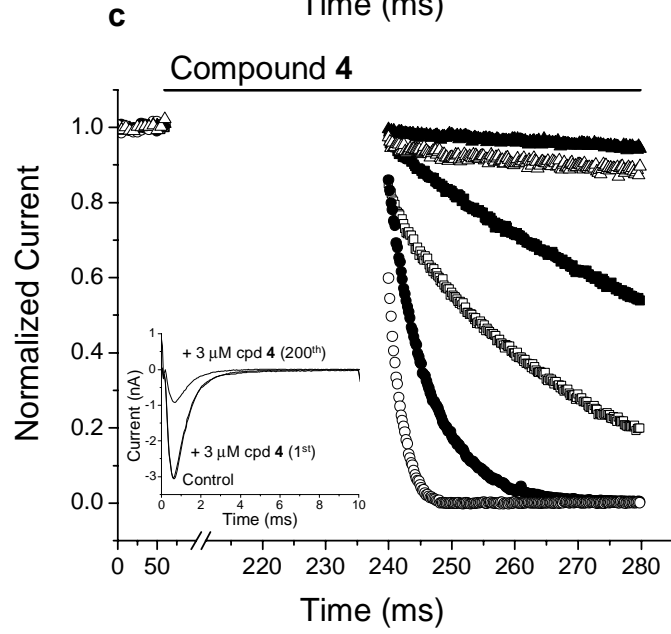
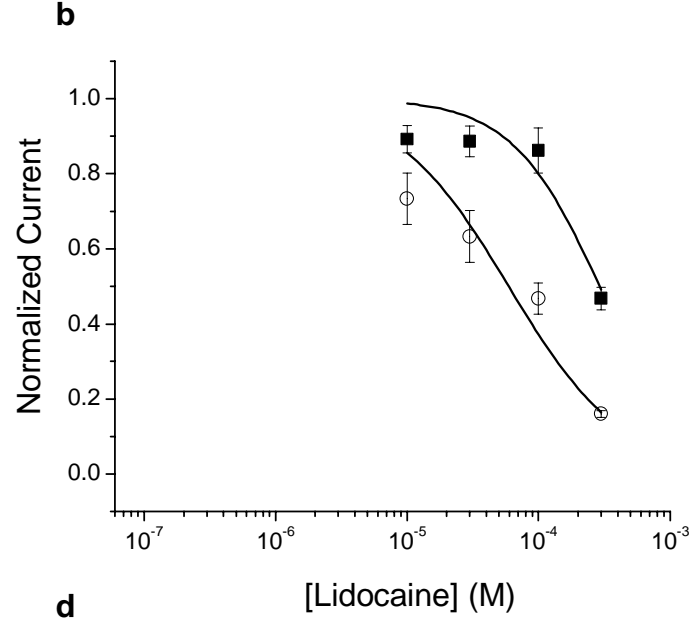
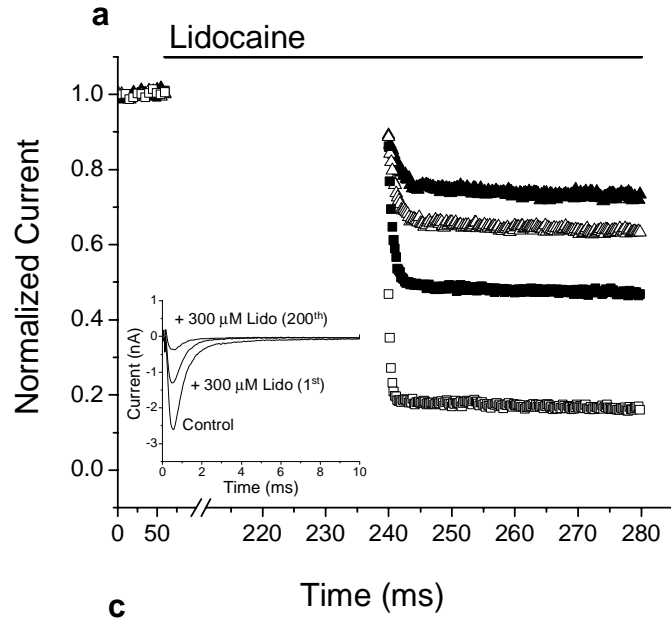


compound 7: $R = H$





3



4

